Handbook of Clinical Neurology, Vol. 176 (3rd series)
Interventional Neuroradiology
S.W. Hetts and D.L. Cooke, Editors
https://doi.org/10.1016/B978-0-444-64034-5.00007-9

Chapter 3

Neurovascular anatomy: Spine

LYDIA GREGG AND PHILIPPE GAILLOUD*

Division of Interventional Neuroradiology and Department of Art as Applied to Medicine, Johns Hopkins University School of Medicine, Baltimore, MD, United States

Abstract

The arterial supply of the spinal cord is provided by the spinal branch of the cervical, thoracic, and lumbar intersegmental arteries. While supply is initially provided at each embryonic segment, only a few prominent anterior radiculomedullary arteries remain at the adult stage, including the arteries of the cervical and lumbosacral enlargements as well as a constant upper thoracic contributor.

The spinal cord is surrounded by the vasocorona, an arterial network that includes several longitudinal anastomotic chains, notably the anterior and posterior spinal arteries, which respectively supply the central and peripheral components of the intrinsic vascularization. The intrinsic venous circulation is also divided into central and peripheral components. The perimedullary venous system includes several longitudinal anastomotic chains interconnected by the coronary plexus. The radiculomedullary veins loosely follow the spinal nerve roots on their way to the epidural plexus. Their point of passage through the thecal sac forms an important valve-like structure, the antireflux mechanism.

INTRODUCTION[1]

Safe and efficient spinovascular procedures require a thorough understanding of spinal vascular anatomy. Spinal digital subtraction angiography (SpDSA) remains the gold standard imaging modality for the evaluation of the spinal vasculature. In addition, endovascular techniques have become a valid minimally invasive option, either as a complement or as an alternative to open surgery. This chapter provides an overview of the vascular anatomy relevant to the performance of diagnostic and therapeutic SpDSA.

DEVELOPMENTAL ANATOMY

The primitive human spinal cord is supplied by paired embryonic dorsal aortae appearing at the six-somite stage (Evans, 1912). Each dorsal aorta provides medial, lateral, and dorsal branches; the latter pass in-between adjacent somites, following an intersegmental rather than segmental distribution (Fig. 3.1) (Evans, 1912).

Each dorsal branch forms a capillary loop with the ipsilateral posterior cardinal vein. This loop reaches the ventrolateral surface of the developing neural tube and anastomoses with adjacent loops to create a network extending to the posterolateral surface of the cord (Evans, 1912). The arterial and venous limbs of the capillary loops become the intersegmental arteries (ISA) and intersegmental veins. The anterior and posterior radicular arteries are early branches of the ISAs (Evans, 1912); they participate in the formation of a plexus on the ventral surface of the cord, from which emerge bilateral longitudinal channels when the embryo is 9 to 11 mm in length (Evans, 1912). These spinal longitudinal channels are continuous with the cranial longitudinal neural arteries (Sabin, 1917). They merge over

[1]Abbreviations used in the chapter are listed at the end of the chapter before References section.

*Correspondence to: Philippe Gailloud, M.D., Division of Interventional Neuroradiology, Johns Hopkins Hospital, 1800 E Orleans Street, Baltimore, MD, 21287, United States. Tel: +1-410-955-8525, Fax: +1-410-614-8238, E-mail: phg@jhmi.edu

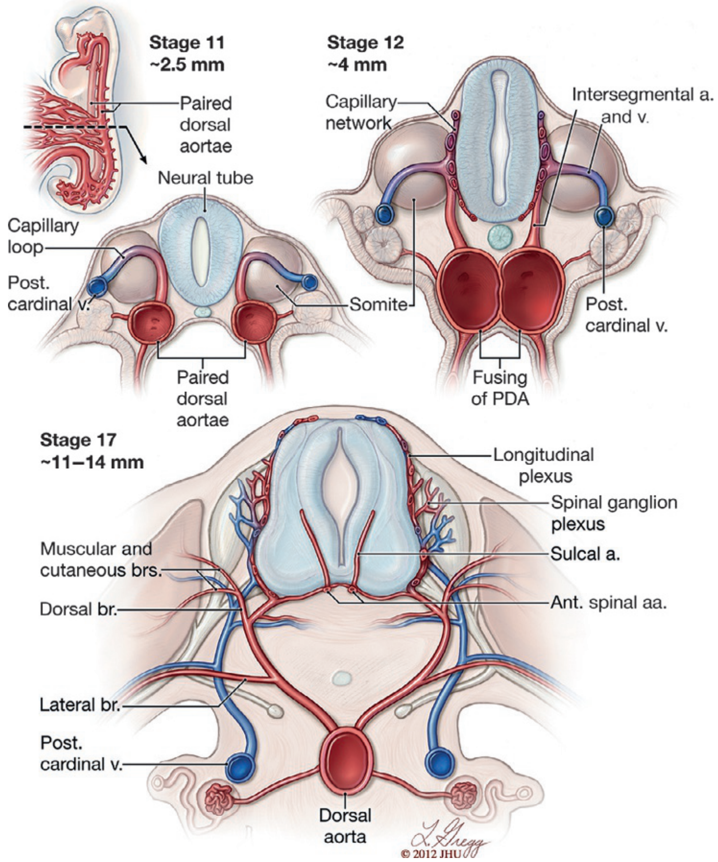

Fig. 3.1. Development of the ISA in the human embryo. Stage 11, the dashed line through the whole embryo clarifies the levels of the subsequent sections. The dorsal branch forms a capillary loop with the ipsilateral posterior cardinal vein in a 2.5-mm embryo. Stage 12, a capillary network then forms along with the anterior and lateral aspects of the neural tube as the primitive aortae begin to fuse in a 4-mm embryo. The arterial side of the capillary loop will develop into the ISAs with corresponding venous drainage at each level. Stage 17, the bilateral radicular branches have formed an anastomotic channel along the anterior aspect of neural tube as the ASAs begin to fuse in an 11- to 14-mm embryo. The dorsal and lateral branches of the adult ISA and the sulcal arteries are now visible. *a.*, artery; aa., arteries; *Ant.*, anterior; *br.*, branch; *brs.*, branches; *PDA*, paired dorsal aortae; *Post.*, posterior; *v.*, vein. Adapted and modified from Evans HM (1912). The development of the vascular system. In: FP Mall, F Keibel (Eds.), In manual of human embryology. J. B. Lippincott Co., Vol. II, Fig. 437, p. 633.

the midline to form the adult anterior spinal artery (ASA) (Evans, 1912), which is the spinal equivalent of the basilar artery formed by the fusion of the longitudinal neural arteries (Charpy, 1899).

The primitive lateral basilovertebral anastomoses of Padget constitute a second pair of longitudinal vessels supplying the developing brainstem; they lie laterally to the longitudinal neural arteries and interconnect the lateral branches of the vertebrobasilar system (Padget, 1948; Padget, 1954; Moffat, 1957). The primitive lateral basilovertebral anastomoses participate in various vertebrobasilar and cerebellar arterial variants (Gregg and Gailloud, 2017).

The development of the posterior spinal arteries (PSA) is slightly delayed but follows a pattern similar to the formation of the ASA. As they lie on the anterior aspect of the dorsal nerve roots, the PSAs fail to fuse into a single channel, keeping a plexiform appearance at the adult stage. The PSAs are continuous with the primitive lateral basilovertebral anastomoses (Thron, 1988).

The earliest and most fundamental component of the ISA is its medial (spinal) contribution (Evans, 1912). The dorsal (muscular) and lateral (intercostal, subcostal, or lumbar) branches are secondary vessels developing later. Depending on their branching pattern, a short common trunk for the spinal and dorsal branches may form, i.e., the dorsospinal artery (Fig. 3.2). The primitive configuration of the ISA with an aortic stem and three branches represents the basic anatomy of the

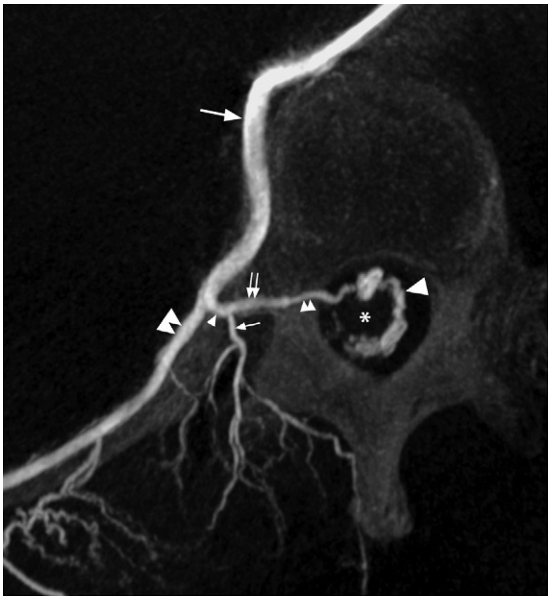

Fig. 3.2. Branches of the ISA three-dimensional SpDSA, left L2 ISA injection, axial maximum intensity projection (MIP) reconstruction in a 44-year-old woman. A typical intersegmental branching pattern is shown, including the ISA trunk (*large arrow*) coming from the aorta and dividing into a lateral (lumbar) branch (*large double arrowhead*) and a dorsospinal artery (*small arrowhead*), which provides a dorsal (muscular) branch (*small arrow*) and a medial (*spinal*) branch (*small double arrows*); in this case, the spinal branch continues as a prominent anterior RMA (*small double arrowhead*) supplying a perimedullary arteriovenous fistula and accounting for the dilatation of the perimedullary venous system (*large arrowhead*). The *asterisk* indicates the location of the spinal cord.

Fig. 3.3. Median sacral artery SpDSA, median sacral artery injection, and posteroanterior projection in a 58-year-old man. The median sacral artery (*arrows*) provides prominent left and right L5 ISAs (*arrowheads*) and connects with the left and right lateral sacral arteries.

adult thoracolumbar ISA. Secondary modification of this pattern at the cervical and sacral levels leads to the formation of the vertebral and sacral arteries. At the cervical level, the V2 segment of the vertebral artery is made of anastomoses linking the first six cervical ISAs and the proatlantal artery (Kadyi, 1889; Congdon, 1922; Padget, 1954).

The fusion of the primitive paired dorsal aortae into a single vessel occurs after the emergence of the embryonic ISAs (Evans, 1912), accounting for the paired distribution of the intersegmental ostia from the posterior aspect of the adult aorta. Misalignment during the fusion process explains how ostia tend to be less strictly aligned transversally than longitudinally, an important fact for spinal angiographers. The true continuation of the adult aorta is the median sacral artery, which typically provides the fifth and, less often, the fourth lumbar ISAs. The common iliac arteries are secondary vessels derived from the umbilical arteries (Broman, 1908; Gest and Carron, 2003) (Fig. 3.3).

THE INTERSEGMENTAL ARTERY AND ITS BRANCHES

Intersegmental artery origins and trunks

The spinal supply originates either directly from ISAs or, at the cervical and sacral levels, from secondary channels that have annexed ISA branches (Congdon, 1922; Padget, 1954). The regional supply can be divided as follows:

(i) Cervicothoracic region: vertebral arteries (ISAs C1-C6) and supreme intercostal arteries (ISAs C7-T2),
(ii) Thoracolumbar region: intercostal, subcostal, and lumbar arteries (ISAs T2-L4),
(iii) Lumbosacral region: iliolumbar artery (L5), median and sacral lateral arteries (S1–S4).

The T3 and L4 ISAs may, respectively, originate from the supreme intercostal or median sacral arteries rather than from the aorta. The ISAs course posteriorly and laterally over the anterior surface of the vertebral column toward their respective neural foramina. Thoracic ISA stems are longer on the right side due to the leftward positioning of the aorta.

Intersegmental trunks can be unilateral or bilateral. Bilateral trunks provide the right and left branches for a single level, they are more common in the lower lumbar region. Unilateral trunks provide branches for two or more adjacent vertebral levels, most often in the upper thoracic region. Complete unilateral trunks include all the intersegmental branches for the levels they supply; incomplete unilateral trunks miss one or more branches, which are provided by a separate ISA. An isolated dorsospinal artery is a classic example of the incomplete unilateral trunk, a relatively common variation that often contributes to the spinal cord supply (Chiras and Merland, 1979; Clavier et al., 1987; Siclari et al., 2006) (Fig. 3.4).

Osseous branches

The vertebral body is supplied by anterolateral and posteromedian osseous branches. The anterolateral arteries come from the intersegmental stem; they are more numerous on the right due to the left-sided position of the aorta (Chiras et al., 1979) and can be divided into ascending, descending, and recurrent branches. The ascending and descending branches form anastomoses with branches from adjacent levels, which can act as collateral pathways. The recurrent branches course medially over the anterior aspect of the vertebral body to anastomose with their contralateral counterparts (Chiras et al., 1979). The anterolateral osseous arteries are responsible for the classic hemivertebral blush observed during selective ISA angiography in adults (Fig. 3.5).

The posteromedian osseous arteries are provided by the retrocorporeal artery, itself stemming from the spinal branch of the ISA. Each retrocorporeal artery divides within the spinal canal into an ascending branch aiming for the corresponding basivertebral foramen and a descending branch for the foramen below, resulting in a diamond-shaped anastomotic network (Fig. 3.6). The posteromedian osseous arteries are responsible for the bilateral vertebral blush seen in children until the retrocorporeal network is supplanted by the anterolateral branches, at about 15 –year old (Ratcliffe, 1982).

The prelaminar arteries also stem from the spinal branch of the ISA and course posteromedially along the posterior vertebral arch to form a second anastomotic network, which can be difficult to differentiate angiographically from the retrocorporeal plexus.

Muscular branches

The dorsal branch of the ISA vascularizes the paraspinal musculature via medial, intermediate, and lateral arteries. The lateral branch of the ISA may also provide paraspinal

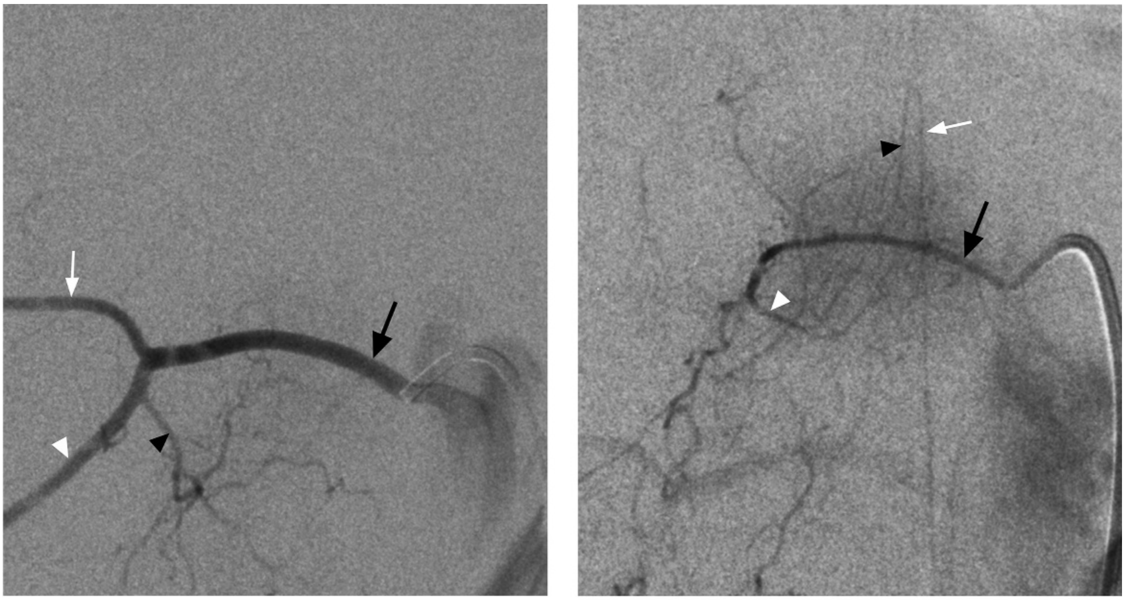

A B

Fig. 3.4. Isolated dorsospinal artery (A) SpDSA, right T11 injection, posteroanterior projection in a 52-year-old woman. The right T11 ISA provides an incomplete unilateral T11–T10 trunk (*black arrow*), with both a lateral (*white arrowhead*) and a dorsospinal (*black arrowhead*) component at T11, but only a lateral branch (*white arrow*) at T10. (B) SpDSA, right T10 injection, posteroanterior projection in the same patient. A diminutive right T10 ISA trunk (*black arrow*) provides an isolated T10 dorsospinal artery (*white arrowhead*), which supplies an anterior RMA (*black arrowhead*) contributing to the ASA (*white arrow*).

Fig. 3.5. Hemivertebral blush SpDSA, right L1 injection, posteroanterior projection in a 55-year-old woman, showing a classic right hemivertebral blush (*asterisk*).

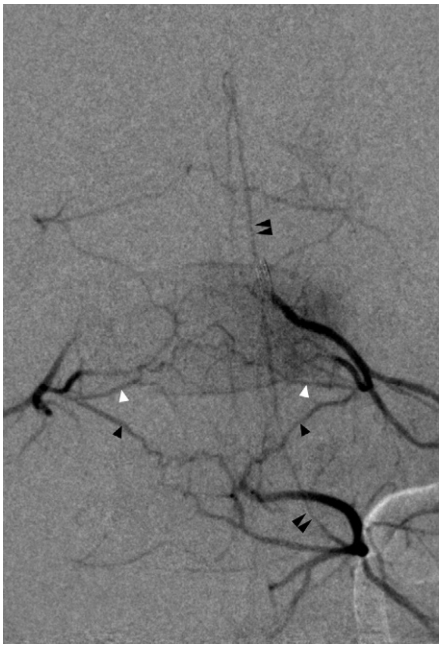

Fig. 3.6. Anastomotic osseous network SpDSA, left T12 injection, posteroanterior projection in a 3-year-old boy documenting the osseous arterial network of the T12 vertebral level. Each retrocorporeal artery divides within the spinal canal into an ascending branch (*white arrowheads*) aiming for the corresponding basivertebral foramen and a descending branch (*black arrowheads*) for the foramen below, resulting in a diamond-shaped anastomotic network. A left L1 anterior RMA (*double black arrowhead*) is also visible.

contributors or anastomose with dorsal branches at the same level. Numerous anastomoses link the muscular and cutaneous branches of adjacent vertebral levels; they represent dangerous collateral pathways during interventional procedures (Gailloud, 2013b). Lumbar ISAs provide additional prominent branches for the psoas muscle (Chiras et al., 1979).

The spinal branch of the intersegmental artery

The posteromedial course of the spinal branch of the ISA follows the nerve root to enter the neural foramen before dividing, when complete, into retrocorporeal, radicular, and prelaminar arteries (Hovelacque, 1937). Radicular and radiculomeningeal branches supply the spinal meninges and nerve root. The radicular artery then passes across the dura to supply the spinal cord, either as a radiculomedullary artery (RMA) connected to a longitudinal spinal artery (ASA and/or PSA) or as a radiculopial artery ending in the vasocorona. As it crosses the neural foramen, the radicular artery most often lies in the anterosuperior quadrant, above the dorsal nerve root (Alleyne et al., 1998; Murthy et al., 2010; Gregg et al., 2017) (Fig. 3.7).

Only a few RMAs remain prominent at the adult stage, 8 anteriorly and 16 posteriorly on average (Kadyi, 1889). A radicular artery may provide both anterior and posterior medullary contributions (artery of Lazorthes) (Lazorthes et al., 1958). The location of functionally significant RMAs in adults is related to the higher metabolic demand of the cervical and lumbosacral enlargements. The cervical spinal cord is supplied by the superior and inferior arteries of the cervical enlargement. The thoracolumbar spinal cord typically relies on a dominant lower thoracic or lumbar anterior RMA, the artery of Adamkiewicz, and a smaller upper thoracic branch, the artery of von Haller (von Haller, 1754; Gailloud, 2013a). The artery of Adamkiewicz originates between T8 and L3 (Djindjian, 1970; Gailloud, 2013a), most often from the left T9 ISA (Rodriguez-Baeza et al., 1991). The artery of von Haller predominantly originates from the left T5 ISA (Gailloud, 2013a). However, significant contributors may be found at any vertebral level (Crock et al., 1986). The caliber of radicular branches that provide a significant anterior RMA artery averages 1.0 mm (Gregg et al., 2017).

The differential growth of the vertebral column and spinal cord results in an apparent ascension of the conus medullaris within the spinal canal; this phenomenon also explains the progressively steeper angle adopted by the radiculomedullary arteries and veins from the cervical to the lumbosacral regions (Fig. 3.8).

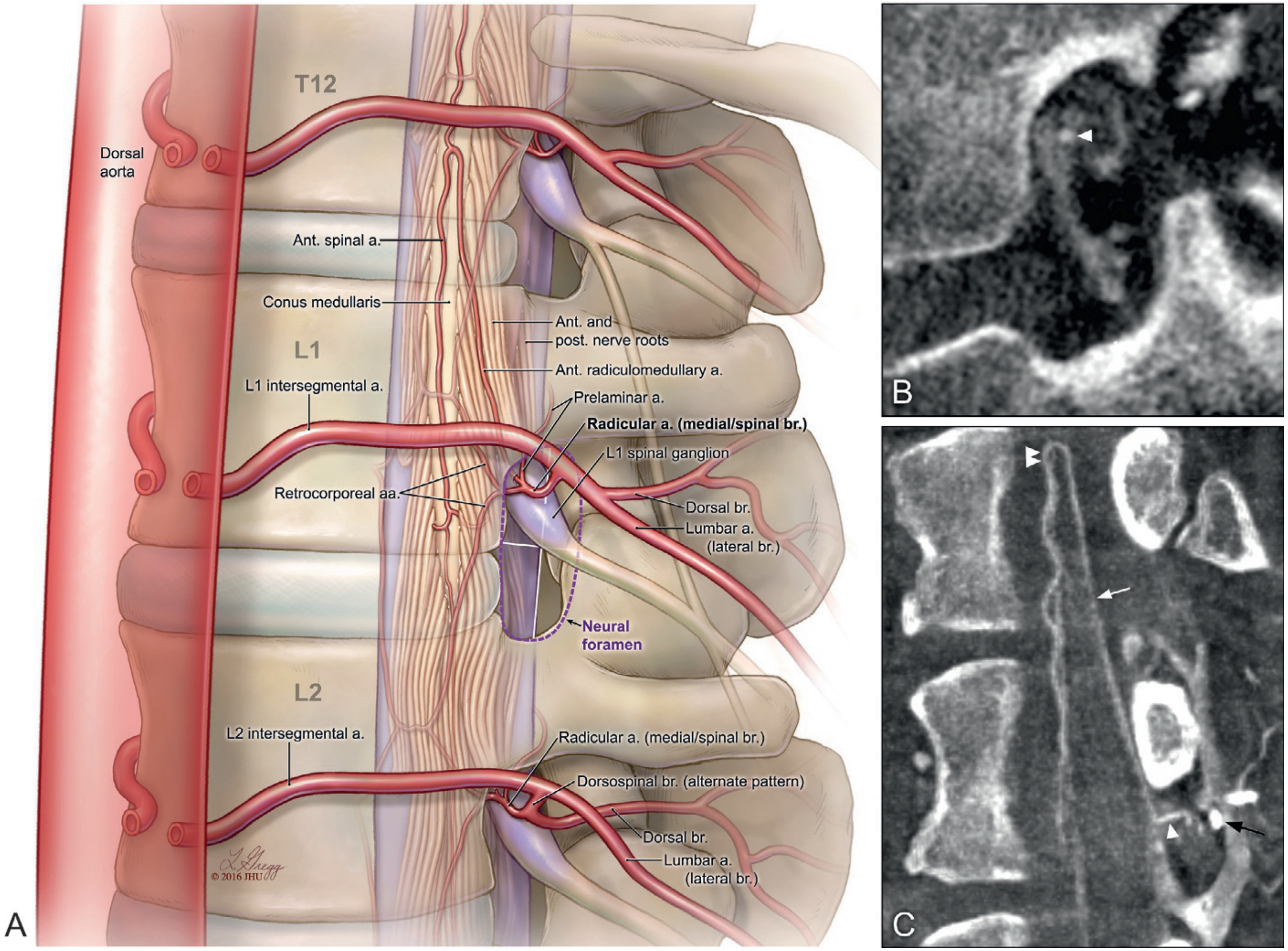

Fig. 3.7. Arterial anatomy of the neural foramen. (A) Anatomy of the ISA (anterior oblique view). A spinal branch enters the left L1 neural foramen and provides retrocorporeal, prelaminar, and radicular arteries; the latter crosses the dura to continue as an anterior RMA supplying the ASA. Anterior RMAs most often lie above the dorsal nerve root, in the anterosuperior quadrant of the foramen. Neural foramen quadrants are indicated by the white gridlines. (B) Flat panel catheter angiotomography (FPCA), left L1 ISA injection, sagittal MIP reconstruction (thickness 0.2 mm) demonstrating the typical position of a radicular artery (*white arrowhead*) within a thoracolumbar neural foramen. (C) FPCA, left L1 ISA injection, anterior oblique MIP reconstruction (thickness 1.5 mm) demonstrating the typical position of a radicular artery (*white arrowhead*) from the left L1 ISA (*black arrow*) within the neural foramen which continues as the anterior RMA (*white arrow*) supplying the ASA (*double white arrowhead*). *a.*, artery; *Ant.*, anterior; *br.*, branch; *post.*, posterior.

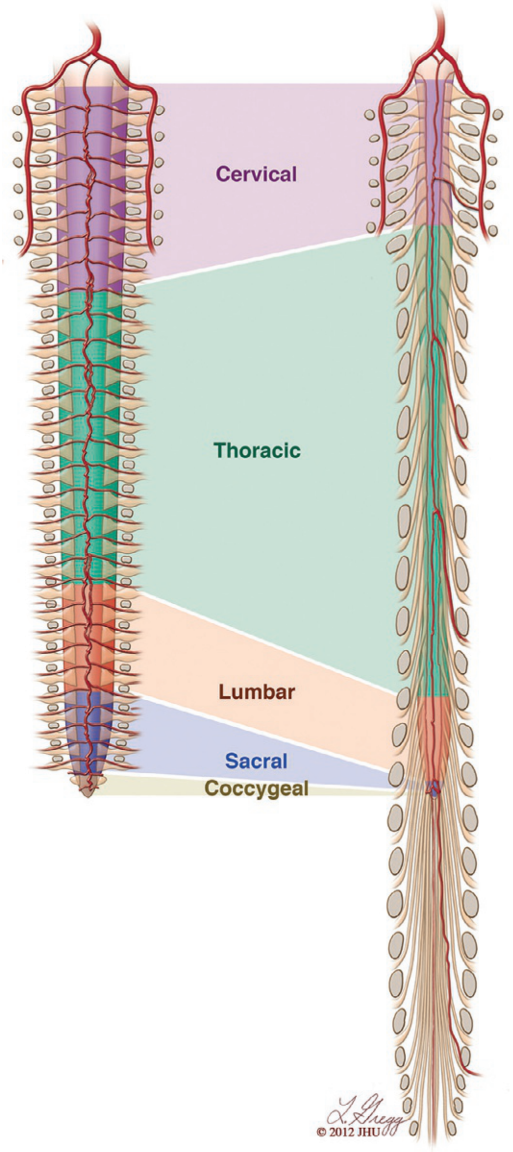

Fig. 3.8. Illustration of spinal cord ascension and elongation within the spinal canal. During early embryonic stages (*left*), the spinal cord occupies the entire length of the spinal canal. As the embryo grows, the spine elongates proportionally more than the spinal cord. In its adult configuration (*right*), the spinal cord fills a smaller portion of the spinal canal and the lumbosacral nerve roots form the cauda equina. Spinal cord segments also grow at different rates, the most pronounced elongation taking place in the thoracic region. This results in a lower longitudinal density of sulcal arteries that may partially account for the increased sensitivity of the thoracic spinal cord to ischemia.

Longitudinal arterial chains of the spinal cord

The vasocorona is an arterial network surrounding the spinal cord, within which nine longitudinal anastomotic chains can be identified (Noeske, 1959) (Fig. 3.9). The most prominent of these chains are the ASA and PSAs; the anterior-lateral and lateral spinal arteries are less conspicuous and less consistent (Fig. 3.10). The ASA is made of a succession of longitudinal anastomoses established between the anterior RMAs of each ISAs. At the adult stage, it appears to originate at the level of the medulla oblongata from the junction of small vertebrospinal trunks provided by each vertebral artery (Fig. 3.11A); it courses caudally, generally uninterrupted, to its termination along the filum terminale (Fig. 3.11B).

The PSAs form in a similar fashion; in adults, they appear to originate from the posterior aspect of the distal vertebral artery, proximal to its dural penetration, or the posterior inferior cerebellar artery (Maillot and Koritke, 1970). Each PSA consists of two parallel channels, the posterior-lateral and posterior-medial spinal arteries (Noeske, 1959), which are immediately ventral and dorsal to the dorsal spinal nerve root origins (Kadyi, 1889; Maillot and Koritke, 1970). The two chains keep an irregular, plexiform appearance (Fig. 3.11C) (Gillilan, 1958; Gailloud et al., 2015).

Near the tip of the conus medullaris, the ASA gives off two small arcuate branches that course laterally and posteriorly to reach the dorsal surface of the cord and anastomose with the caudal end of the posterior spinal chains to constitute the periconal anastomotic circle (Henle, 1868; Kadyi, 1889) (Fig. 3.11B). Under normal circumstances, the direction of flow in the periconal anastomotic circle is craniocaudal in the distal ASA and caudocranial in the distal PSAs (Bolton, 1939; Di Chiro and Fried, 1971). This flow pattern creates a zone of shared supply, a “watershed territory,” in the dorsal lumbosacral region (Gailloud et al., 2015) (Fig. 3.12). The direction of flow can be reversed when the circle acts as a source of collateral supply.

Intrinsic arteries of the spinal cord

The longitudinal arterial chains and the vasocorona supply the spinal gray and white matter. As noted by Adamkiewicz, the ASA supplies the central (or centrifugal) circulation via sulcal arteries that enter the anterior-median fissure, while perforating branches of the PSAs and vasocorona provide the peripheral (or centripetal) cord supply (Adamkiewicz, 1882). The two circulations overlap, creating an area of shared supply (i.e., a watershed territory) (Turnbull, 1971). However, neither the vasocorona nor the intramedullary anastomoses between the central and peripheral circulations represent meaningful sources of collateral supply (Lazorthes et al., 1973).

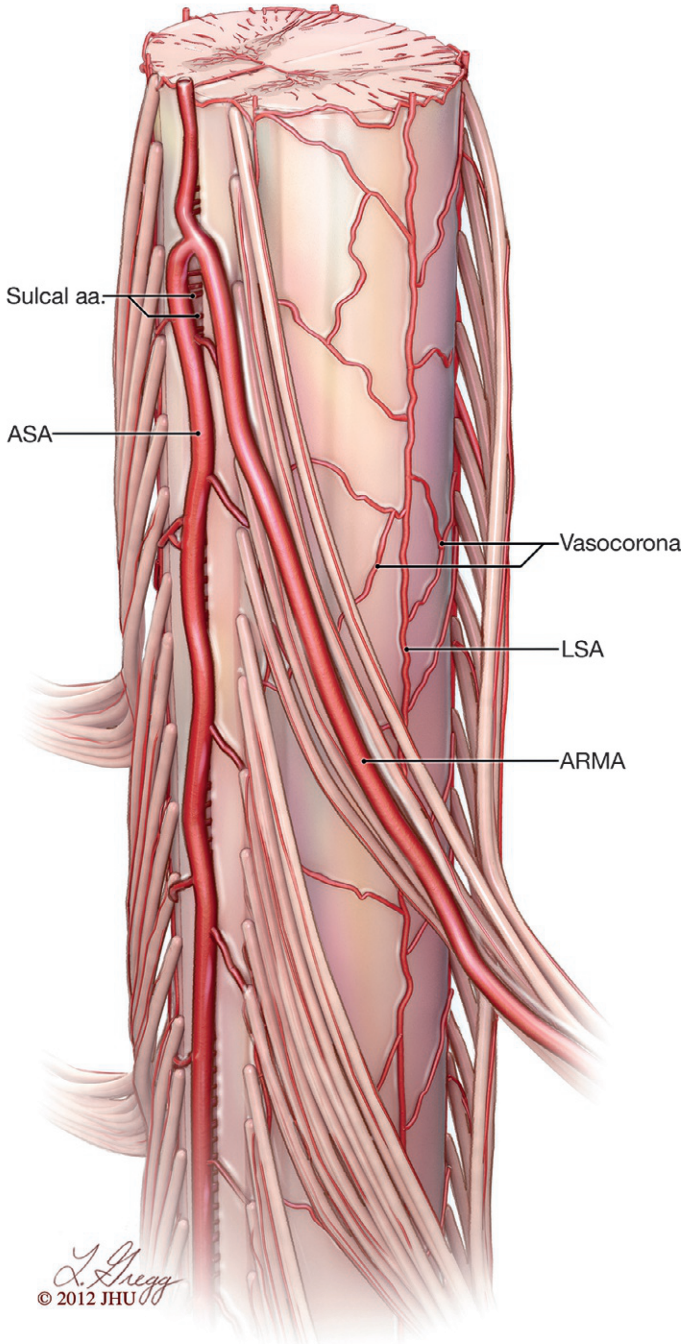

Fig. 3.9. The superficial spinal arterial system (thoracic level). This illustration depicts a prominent anterior RMA, the anterior and lateral longitudinal spinal arterial chains, and the vasocorona. *a.*, artery; *aa.*, arteries; *ASA*, anterior spinal artery; *LSA*, lateral spinal artery.

As the sulcal arteries reach the depth of the anterior-median fissure, they divide into sulcocommissural branches (Adamkiewicz, 1882), which typically have a unilateral distribution with alternating left and right branches (Kadyi, 1889; Herren and Alexander, 1939). This arrangement can be attributed to the paired origin of the ASA; each primitive chain originally supplies the ipsilateral side of the neural tube (Fig. 3.1) (Evans, 1912). Sulcal arteries less commonly form trunks with multiple unilateral or bilateral branches (Hassler, 1966; Zhang et al., 1997). Branches of the sulcocommissural arteries are almost exclusively limited to the gray matter (Zhang et al., 1997).

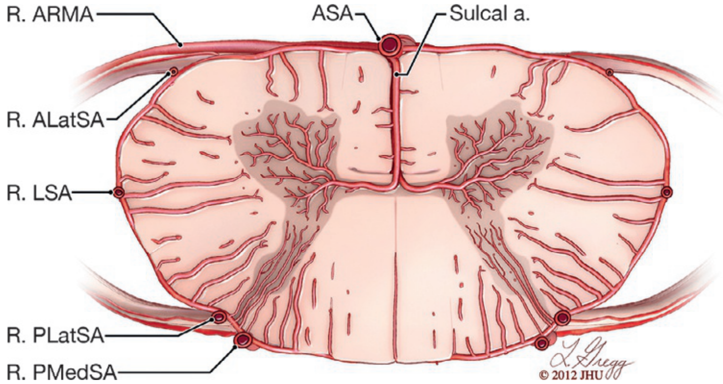

Fig. 3.10. The longitudinal spinal arterial chains (cervical level, axial view). The image depicts the relatively constant primary chains, the ASA and PSAs, each PSA with a posterior-lateral and a posterior-medial artery. Secondary chains include the paired anterior-lateral and lateral spinal arteries, which are less conspicuous and less constant. *a.*, artery; *ALatSA*, anterior-lateral spinal artery; *LSA*, lateral spinal artery; *PLatSA*, posterior-lateral spinal artery; *PMedSA*, posterior-medial spinal artery; *R.*, right.

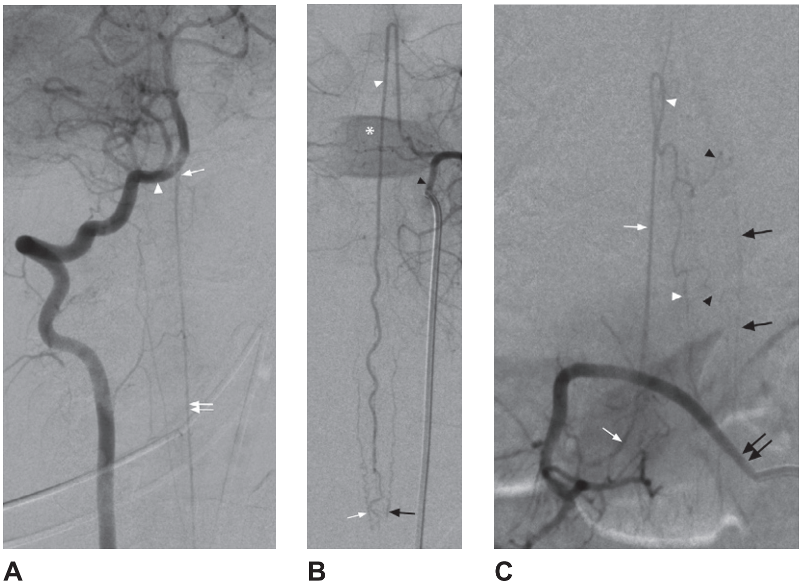

Fig. 3.11. The anterior and posterior spinal arteries. (A) DSA, right vertebral artery injection, posteroanterior projection, documenting the cervical ASA in a 25-year-old woman. In this case, the ASA originates from a robust right vertebrospinal trunk (*arrow*) provided by the vertebral artery (*arrowhead*) and continues inferiorly (*double arrow*) along the anterior-median fissure of the spinal cord. (B) SpDSA, left T9 injection, posteroanterior projection, documenting the principal supply to the thoracolumbar spinal cord and the periconal arterial circle in a 7-year-old boy. The left T9 ISA (*black arrowhead*) supplies the ASA (*white arrowhead*). Near the tip of the conus medullaris, the ASA gives off two small arcuate branches that course laterally and posteriorly to reach the dorsal surface of the cord and anastomose with the caudal end of the left (*black arrow*) and right (*white arrow*) PSAs to constitute the periconal anastomotic circle (Henle, 1868; Kadyi, 1889). A bilateral vertebral blush, typical of children, is also documented (*asterisk*). (C) SpDSA, right L1 injection, posteroanterior projection, documenting the PSAs in a 56-year-old man. The L1 ISA (*double black arrow*) provides a posterior radiculomedullary artery (*white arrows*) that connects to the right posterior-lateral spinal artery (*white arrowheads*). Plexiform vessels form a network (*black arrowheads*) that connects with the contralateral PSAs (*black arrows*).

The longitudinal density of sulcal arteries is the lowest in the thoracic cord and the highest in the lumbosacral cord (Lazorthes et al., 1958; Hassler, 1966; Zhang et al., 1997), a difference caused by the more pronounced elongation of the thoracic cord during development (Lazorthes et al., 1957) (Fig. 3.8). Sulcal arteries also tend to take a superior-oblique course within the anterior-median fissure in the thoracic and cervical regions (Hassler, 1966). In the thoracic region, the reduced number of radicular contributions, their smaller diameter, and

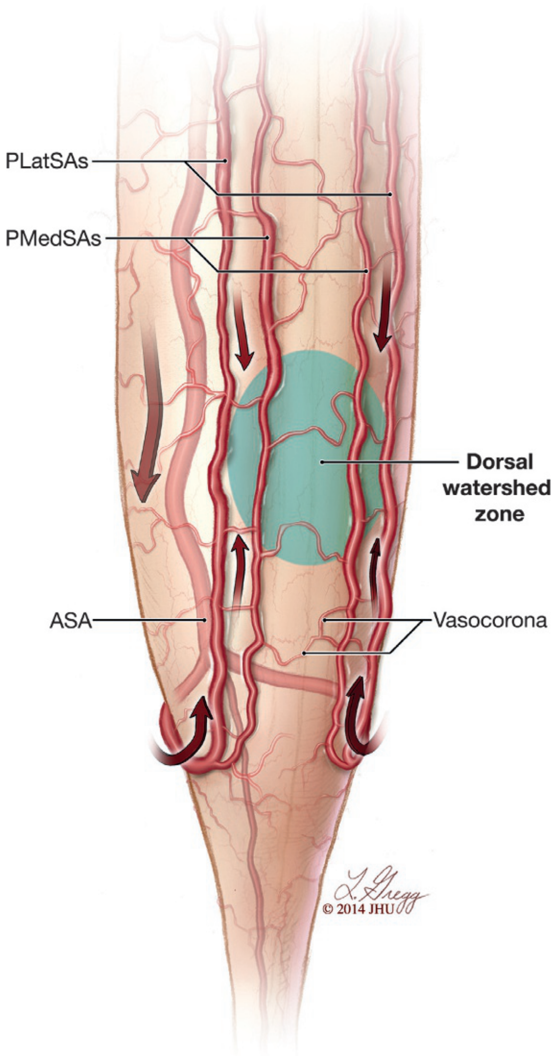

Fig. 3.12. The dorsal watershed zone of the spinal cord. The blood flow in the caudal segments of the posterior-lateral and posterior-medial spinal arteries, which are supplied by the arcuate branches of the ASA, is ascending while the flow direction in the more cranial portion of the PSAs is descending. This flow pattern creates an area of shared supply, the dorsal watershed zone (*shaded green area*). *ASA*, anterior spinal artery; *PLatSAs*, posterior-lateral spinal arteries; *PMedSAs*, posterior-medial spinal arteries.

the increased distance between sulcal arteries (Hassler, 1966) may contribute to the thoracic cord sensitivity to ischemia (Herren and Alexander, 1939; Hassler, 1966).

VENOUS ANATOMY OF THE SPINAL CORD

Intrinsic venous drainage

The intramedullary venous network is, like the intrinsic arterial circulation, divided into central and peripheral components (Fig. 3.13A). The paracentral veins collect blood from the central gray matter and drain into sulcal veins, which receive additional tributaries from the anterior and median parenchyma (Gillilan, 1970) before terminating into the anteromedian spinal vein. Adjacent sulcal veins can form longitudinal anastomotic chains, either within the central gray matter (paracentral longitudinal anastomosis) or the anterior-median fissure (sulcal longitudinal anastomosis) (Gillilan, 1970). Paracentral longitudinal anastomoses can participate in the development of spinal developmental venous anomalies (Pearl et al., 2012).

The white and posterior gray matters primarily drain into peripheral veins that course radially toward the coronary plexus. Peripheral veins that drain the anterior and posterior radicular fasciculi are more robust (Lazorthes et al., 1973). The septal veins, located in the posterior-median fissure, terminate into the posteromedian spinal vein.

Transmedullary venous anastomoses (TMVA) assume two primary configurations. Centrodorsolateral anastomoses (Fig. 3.13B) are formed by a connection between a sulcal and a paracentral vein; their oblique transmedullary segment interconnects the anteromedian spinal vein to an ipsilateral posterolateral spinal vein (Herren and Alexander, 1939; Crock and Yoshizawa, 1977). Median anteroposterior anastomoses (Fig. 3.13C) are made of a connection between a sulcal and a septal vein linking the anteromedian and posteromedian spinal veins (Crock and Yoshizawa, 1977). Other configurations, such as combined centrodorsolateral and median anteroposterior TMVAs, have been reported (Gregg and Gailloud, 2015). TMVAs may help regulate venous drainage and pressure by allowing rapid flow between the anterior and posterior venous circulations (Herren and Alexander, 1939). Clinically, TMVAs may be confused with vascular malformations or intramedullary hemorrhages on noninvasive imaging, and they can be used as an access route for endovascular therapy (Giese et al., 2010).

Extrinsic venous drainage

The perimedullary venous system includes several longitudinal venous chains interconnected by the coronary plexus (Kadyi, 1889). The larger anteromedian and posteromedian spinal veins, respectively, course over the anterior-median and posterior-median fissures, while the smaller paired posterolateral spinal veins lie behind the dorsal spinal nerve rootlets, close to the PSAs (Suh and Alexander, 1939; Zhang et al., 1997) (Fig. 3.14). The anteromedian spinal vein is located deep or lateral to the ASA (Dommisse, 1975). The posteromedian spinal vein is usually dominant, notably in the lower thoracolumbar region; it has a serpentine course, with occasional plexiform segments (Tadie et al., 1985). A few large superficial anastomoses connect the anterior and posterior venous circulation (Kadyi, 1889; Suh and Alexander, 1939).

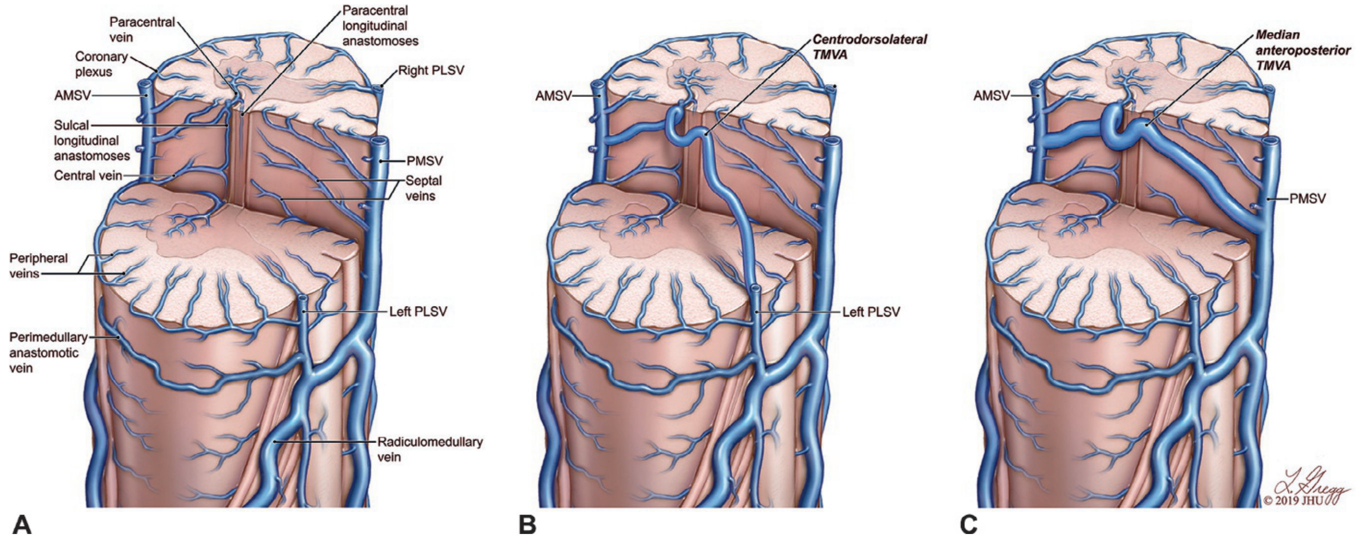

Fig. 3.13. The spinal venous system. (A) The paracentral veins collect blood from the central gray matter and drain into central veins, which terminate into the anteromedian spinal vein. Adjacent central veins can form longitudinal anastomotic chains, either within the central gray matter (paracentral longitudinal anastomosis) or the anterior-median fissure (sulcal longitudinal anastomosis) (Gillilan, 1970). The white matter and posterior gray matter primarily drain into peripheral veins that course radially toward the coronary plexus. The septal veins, located in the posterior-median fissure, terminate into the posteromedian spinal vein. (B) Centrodorsolateral transmedullary venous anastomoses are formed by enlarged central and paracentral veins with an oblique transmedullary segment that connects to an ipsilateral posterolateral spinal vein. (C) Median anteroposterior transmedullary anastomoses are made by a connection between enlarged central and septal veins interconnecting the anteromedian and posteromedian spinal veins, with a typical loop around the central canal. *AMSV*, anterior-median spinal vein; *PLSV*, posterior-lateral spinal vein; *PMSV*, posterior-median spinal vein; *TMVA*, transmedullary venous anastomoses.

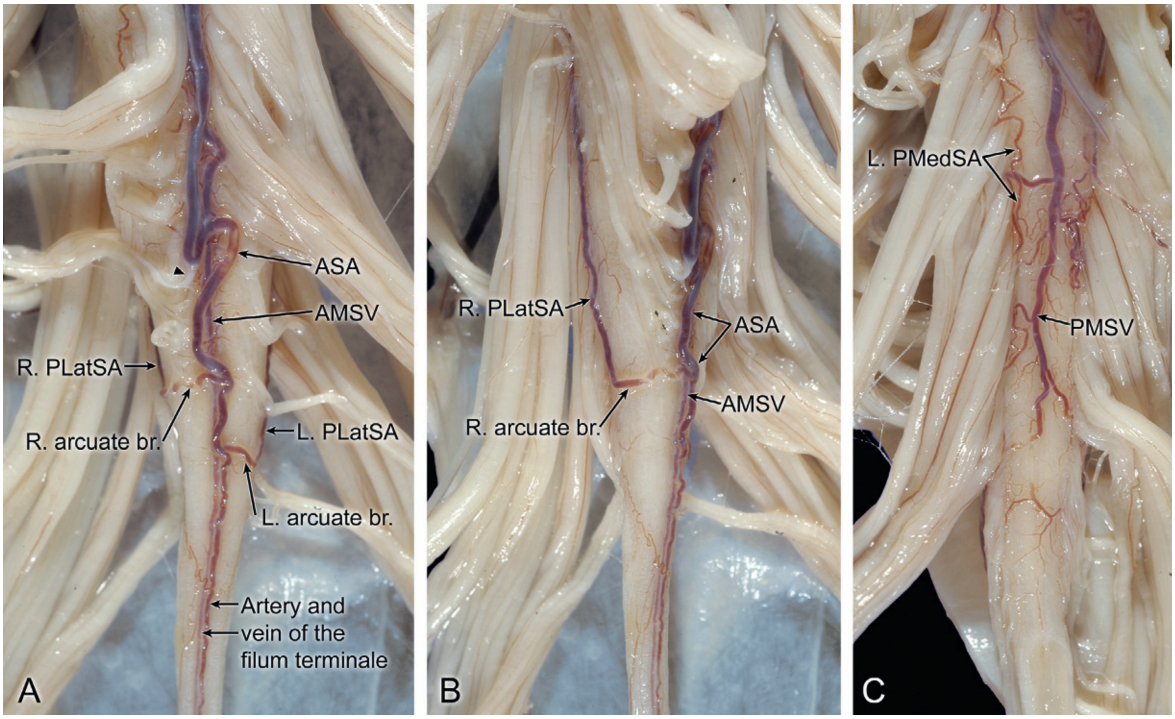

Fig. 3.14. Periconal arterial and venous anatomy. (A) Photograph, anterior view of an adult conus medullaris; the ASA courses along the anterior-median fissure, by the side or above the anterior-median spinal vein. The arcuate branches course laterally and posteriorly to reach the dorsal surface of the cord and anastomose with the caudal end of the posterior-lateral spinal arteries, constituting the periconal anastomotic circle. The artery and vein of the filum terminale and a remnant of an obliterated radiculomedullary artery (*black arrowhead*) are also visible. (B) Lateral view showing the right arcuate branch anastomosing with the caudal end of the right posterior-lateral spinal artery. The right ventral nerve rootlets of the cauda equina have been reflected cranially. (C) Posterior view showing the posterior-median spinal vein and the posterior-medial spinal arteries. *AMSV*, anterior-median spinal vein; *br.*, branch; *L.*, left; *PMedSV*, posterior-median spinal vein; *PLatSV*, posterior-lateral spinal vein; *R.*, right.

A variable number of radiculomedullary veins drain the perimedullary venous system: 3 to 5 are located dorsally, 2 to 3 ventrally (Tadie et al., 1985). The radiculomedullary veins loosely follow the ventral and dorsal nerve roots (Dommisse, 1975; Tadie, 1979), often skipping a vertebral level before exiting the thecal sac. Numerous smaller veins extend from the venous plexuses of the spinal ganglia to the nerve rootlets to drain into the perimedullary venous network (Tadie et al., 1985).

As they cross the thecal sac, radiculomedullary veins assume a short oblique course in between the two layers of the dura before reaching the epidural venous plexus (Tadié et al., 1978; Tadie, 1979). This configuration, known as the antireflux mechanism, acts as a pseudovalve that prevents retrograde radiculomedullary flow during acute or chronic pressure increases in the epidural plexus (Crock and Yoshizawa, 1977; Tadié et al., 1978; Tadie et al., 1985; Gailloud, 2014) (Fig. 3.15). The epidural plexus is connected to the external vertebral venous system by emissary veins accompanying the spinal nerves through the neural foramina.

Radiculomedullary veins may originate from the perimedullary venous network as single vessels or as

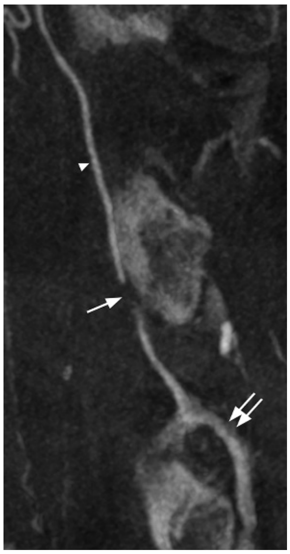

Fig. 3.15. The antireflux mechanism FPCA, left L1 injection, coronal MIP reconstruction, documenting a focal narrowing (*arrow*) where the radiculomedullary vein (*arrowhead*) crosses the thecal sac on its way to the epidural plexus (*double arrow*).

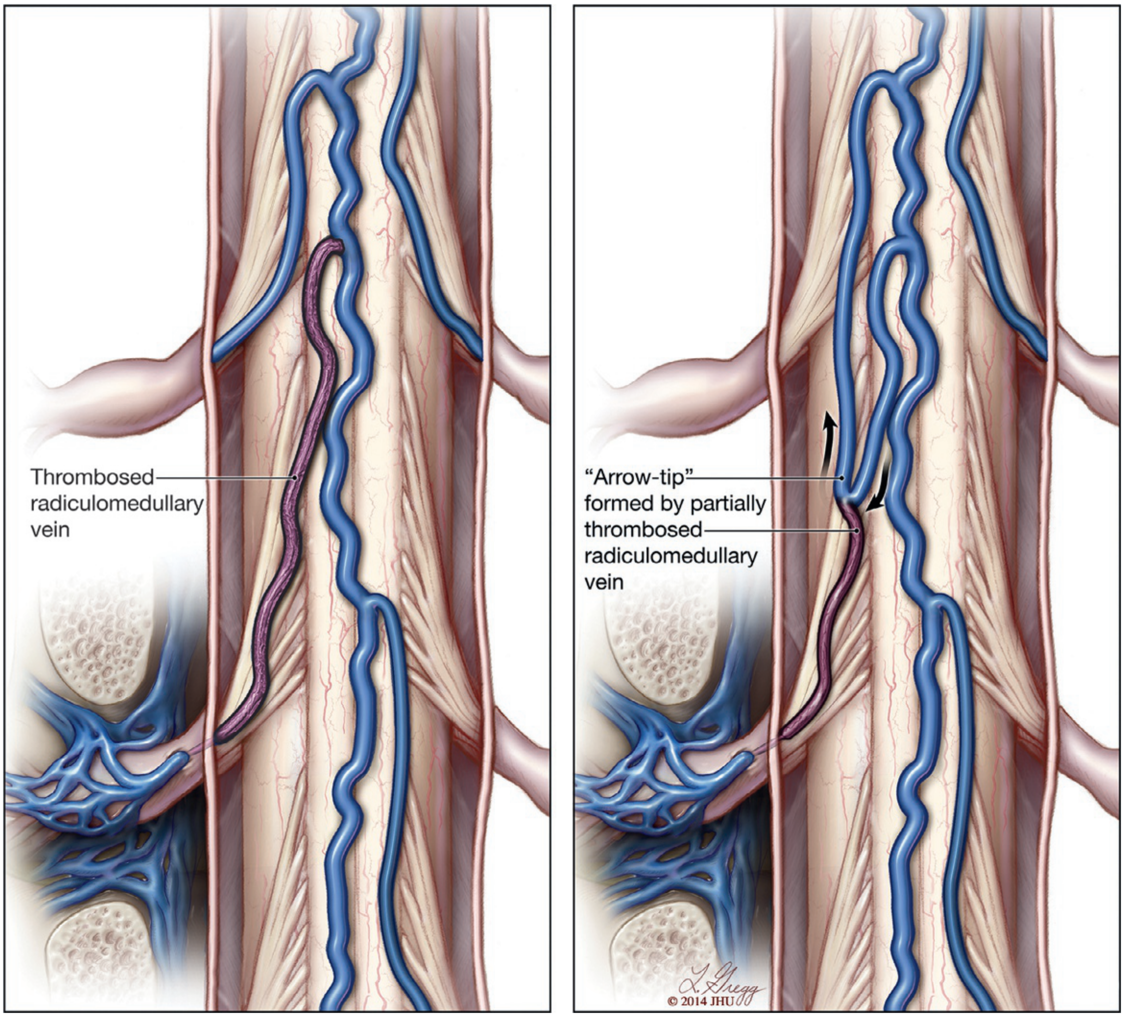

Fig. 3.16. Radiculomedullary vein thrombosis and "arrow-tipped" loops (*posterior view*). Radiculomedullary veins originate from the perimedullary venous network and drain into the epidural venous plexus. The left image depicts a completely thrombosed single-rooted radiculomedullary vein. In the right image, the distal segment of a radiculomedullary vein has thrombosed but, because of its dual-rooted configuration, its proximal segment remains patent, forming a so-called "arrow-tipped loop."

dual venous channels that fuse before reaching the dura (Tadié et al., 1978). An "arrow-tipped loop" is formed when the distal component of a radiculomedullary vein with a dual-origin is not patent; the vein then appears to rebound on the inner surface of the thecal sac and interconnect two segments of the perimedullary venous system (Kadyi, 1889; Crock and Yoshizawa, 1977) (Fig. 3.16). Rather than a normal variant, arrow-tipped loops are likely formed by thrombosis of the terminal segment of a radiculomedullary vein with dual origin and constitute an angiographic marker of spinal venous thrombosis (Gailloud, 2014).

ABBREVIATIONS

ASA, anterior spinal artery; FPCA, flat panel catheter angiotomography; ISA, intersegmental arteries; MIP, maximum intensity projection; PSA, posterior spinal artery; RMA, radiculomedullary arteries; SpDSA, spinal digital subtraction angiography; TMVA, transmedullary venous anastomoses.

References

Adamkiewicz A (1882). 'Die Blutgefässe des menschlichen Rückenmarkes. II. Theil. Die Gefässe der Rückenmarks-Oberfläche. In: Sitzungsberichten der Kaiserlichen Akademie der Wissenschaften, Mathematisch-naturwissensc-haftliche Classe, 85: 101–130.

Alleyne Jr CH, Cawley CM, Shengelaia GG et al. (1998). Microsurgical anatomy of the artery of Adamkiewicz and its segmental artery. J Neurosurg 89 (5): 791–795.

Bolton B (1939). The blood supply of the human spinal cord. J Neurol Psychiatry 2 (2): 137–148.

Broman I (1908). Über die entwickelung und “wanderung” der zweige der aorta abdominalis beim menschen. Anat Embryol 36 (3): 405–550.

Charpy A (1899). Vaisseaux des Centres Nerveux. In: P Poirier, A Charpy (Eds.), Traité d’Anatomie Humaine. Masson et Cie, Éditeurs, Paris, pp. 549–610.

Chiras J, Merland J (1979). The dorsospinal artery. A little known anatomical variant. Its importance in spinal angiography. J Neuroradiol 6 (2): 93.

Chiras J, Morvan G, Merland J (1979). The angiographic appearances of the normal intercostal and lumbar arteries. Analysis and the anatomic correlation of the lateral branches. J Neuroradiol 6 (3): 169–196.

Clavier E, Guimaraems L, Chiras J et al. (1987). Isolated dorsospinal artery supplying anterior spinal artery. Neuroradiology 29 (2): 213.

Congdon ED (1922). Transformation of the aortic-arch system during the development of the human embryo. Contributions to Embryology. Carnegie Institution of Washington publication, no. 277. 14 (68): 47–110.

Crock HV, Yoshizawa H (1977). The blood supply of the vertebral column and spinal cord in man, Springer-Verlag, New York.

Crock HV, Yamagishi M, Crock MC (1986). The conus medullaris and cauda equina in man: an atlas of the arteries and veins, Springer.

Di Chiro G, Fried LC (1971). Blood flow currents in spinal cord arteries. Neurology 21 (11): 1088.

Djindjian R (1970). Angiography of the spinal cord, University Park Press.

Dommisse GF (1975). The arteries and veins of the human spinal cord from birth, Churchill Livingstone.

Evans HM (1912). The development of the vascular system. In: FP Mall, F Keibel (Eds.), In manual of human embryology. J. B. Lippincott Co., pp. 570–709.

Gailloud P (2013a). The artery of von Haller: a constant anterior radiculomedullary artery at the upper thoracic level. Neurosurgery 73 (6): 1034–1043.

Gailloud P (2013b). Chapter 88: arterial anatomy of the spine and spinal cord. In: MA Mauro, KP Murphy, KR Thomson, AC Venbrux, RA Morgan (Eds.), Image-Guided Interventions E-Book: Expert Radiology Series. Elsevier Health Sciences.

Gailloud P (2014). The arrow-tipped loop is a marker of radiculomedullary vein thrombosis linked to the anti-reflux mechanism—angiographic anatomy and clinical implications. Neuroradiology 56 (10): 859–864.

Gailloud P, Gregg L, Galan P et al. (2015). Periconal arterial anastomotic circle and posterior lumbosacral watershed zone of the spinal cord. J NeuroInterven Surg 7: 848–853.

Gest TR, Carron MA (2003). Embryonic origin of the caudal mesenteric artery in the mouse. Anat Rec 271 (1): 192–201.

Giese A, Winkler PA, Schichor C et al. (2010). A transmedullary approach to occlusion of a ventral perimedullary arteriovenous fistula of the thoracic spinal cord. Neurosurgery 66 (3): 611–615.

Gillilan LA (1958). The arterial blood supply of the human spinal cord. J Comp Neurol 110 (1): 75–103.

Gillilan LA (1970). Veins of the spinal cord. Anatomic details; suggested clinical applications. Neurology 20 (9): 860–868.

Gregg L, Gailloud P (2015). Transmedullary venous anastomoses: anatomy and angiographic visualization using flat panel catheter angiotomography. AJNR Am J Neuroradiol 36 (7): 1381–1388.

Gregg L, Gailloud P (2017). The role of the primitive lateral basilovertebral anastomosis of padget in variations of the vertebrobasilar arterial system. Anat Rec (Hoboken) 300 (11): 2025–2038.

Gregg L, Sorte D, Gailloud P (2017). Intraforaminal location of thoracolumbar radicular arteries providing an anterior radiculomedullary artery using flat panel catheter angiotomography. Am J Neuroradiol 38 (5): 1054–1060.

Hassler O (1966). Blood supply to human spinal cord: a microangiographic study. Arch Neurol 15 (3): 302–307.

Henle J (1868). Handbuch der Gefässlehre des Menschen, Friedrich Vieweg und Sohn, Braunschweig.

Herren RY, Alexander L (1939). Sulcal and intrinsic blood vessels of the human spinal cord. Arch Neurol Psychiatry 41 (4): 678–687.

Hovelacque A (1937). Le thorax, anatomie médico-chirurgicale, Maloine, Paris.

Kadyi H (1889). Über die Blutgefässe des Menschlichen Rückenmarkes, Gubryonowisz & Schmidt, Lemberg, Poland.

Lazorthes G, Poulhes J, Bastide G et al. (1957). Recherches sur la vascularisation artérielle de la moelle. Applications à la pathologie médullaire. Bull Acad Natl Med 141 (21 – 23): 464–477.

Lazorthes G, Poulhes J, Bastide G et al. (1958). La vascularisation artérielle de la moelle. Recherches anatomiques et applications à la pathologie médullaire et à la pathologie aortique. Neurochirurgie 4: 3–19.

Lazorthes G, Gouaze A, Djindjian R (1973). Vascularisation et circulation de la moelle épinière, Masson & Cie, Paris.

Maillot C, Koritke JG (1970). Origins of the posterior spinal artery trunk in man. C R Assoc Anat 149: 837–847.

Moffat DB (1957). The development of the hindbrain arteries in the rat. J Anat 91: 25–39.

Murthy NS, Maus TP, Behrns CL (2010). Intraforaminal location of the great anterior radiculomedullary artery (artery of Adamkiewicz): a retrospective review. Pain Med 11 (12): 1756–1764.

Noeske K (1959). Über die arterielle Versorgung des menschlichen Rückenmarkes. Morphol Jahrb 99: 455–497.

Padget DH (1948). The development of cranial arteries in the human embryo. Contr Embryol Carneg Inst 32: 205–261.

Padget DH (1954). Designation of the embryonic intersegmental arteries in reference to the vertebral artery and subclavian stem. Anat Rec 119: 349–356.

Pearl MS, Chen JX, Gregg L et al. (2012). Angiographic detection and characterization of “cryptic venous anomalies” associated with spinal cord cavernous malformations using flat-panel catheter angiotomography. Neurosurgery 71: 125–132.

Ratcliffe J (1982). An evaluation of the intra-osseous arterial anastomoses in the human vertebral body at different ages. A microarteriographic study. J Anat 134: 373.

Rodriguez-Baeza A, Muset-Lara A, Rodriguez-Pazos M et al. (1991). The arterial supply of the human spinal cord: a new approach to the arteria radicularis magna of Adamkiewicz. Acta Neurochir 109 (1–2): 57–62.

Sabin F (1917). Origin and development of the primitive vessels of the chick and of the pig, Carnegie Institution of Washington Publication.

Siclari F, Fasel JH, Gailloud P (2006). Direct emergence of the dorsospinal artery from the aorta and spinal cord blood supply. Neuroradiology 48: 412–414.

Suh T, Alexander L (1939). Vascular system of the human spinal cord. Arch Neurol Psychiatry 41 (4): 659–677.

Tadie M (1979). Le dispositif protecteur antireflux des veins de la moelle. Neurochirurgie 25: 28–30.

Tadié M, Hemet J, Aaron C et al. (1978). Les veines radiculaires de drainage de la moelle ont-elles un dispositif de sécurité anti-reflux. Bull Acad Natl Med 162: 550–554.

Tadie M, Hemet J, Freger P et al. (1985). Morphological and functional anatomy of spinal cord veins. J Neuroradiol 12 (1): 3–20.

Thron A (1988). Vascular anatomy of the spinal cord. In: Neuroradiological Investigations and Clinical Syndromes, Springer-Verlag, Wien New York.

Turnbull IM (1971). Microvasculature of the human spinal cord. J Neurosurg 35 (2): 141–147.

von Haller A (1754). Iconum anatomicarum quibus aliquae partes corporis humani delineatae traduntur. Fasciculus VII—Arteriae cerebri Medullae spinalis Oculi, Widow of Abram Vandenhoeck, Göttingen, Germany.

Zhang Z-A, Nonaka H, Hatori T (1997). The microvasculature of the spinal cord in the human adult. Neuropathology 17 (1): 32–42.